Molecular Therapy
Nucleic Acids
Original Article

BMP4 Upregulation Is Associated with Acquired Drug Resistance and Fatty Acid Metabolism in EGFR-Mutant Non-Small-Cell Lung Cancer Cells

Duc-Hiep Bach,[1] Thi-Thu-Trang Luu,[1] Donghwa Kim,[1] Yong Jin An,[1] Sunghyouk Park,[1] Hyen Joo Park,[1] and Sang Kook Lee[1]

[1]College of Pharmacy, Natural Products Research Institute, Seoul National University, Seoul 151-742, South Korea

Lung cancer is the leading cause of cancer-associated deaths worldwide. In particular, non-small-cell lung cancer (NSCLC) cells harboring epidermal growth factor receptor (EGFR) mutations are associated with resistance development of EGFR tyrosine kinase inhibitor (EGFR-TKI) treatment. Recent findings suggest that bone morphogenetic proteins (BMPs) and microRNAs (miRNAs) might act as oncogenes or tumor suppressors in the tumor microenvironment. In this study, for the first time, we identified the potential roles of BMPs and miRNAs involved in EGFR-TKI resistance by analyzing datasets from a pair of parental cells and NSCLC cells with acquired EGFR-TKI resistance. BMP4 was observed to be significantly overexpressed in the EGFR-TKI-resistant cells, and its mechanism of action was strongly associated with the induction of cancer cell energy metabolism through the modulation of Acyl-CoA synthetase long-chain family member 4. In addition, miR-139-5p was observed to be significantly downregulated in the resistant NSCLC cells. The combination of miR-139-5p and yuanhuadine, a naturally derived antitumor agent, synergistically suppressed BMP4 expression in the resistant cells. We further confirmed that LDN-193189, a small molecule BMP receptor 1 inhibitor, effectively inhibited tumor growth in a xenograft nude mouse model implanted with the EFGR-TKI-resistant cells. These findings suggest a novel role of BMP4-mediated tumorigenesis in the progression of acquired drug resistance in EGFR-mutant NSCLC cells.

INTRODUCTION

The rapid emergence of resistance to chemotherapy and molecular targeted therapies is currently considered a major reason for treatment failure in cancer patients.[1–3] Various molecular mechanisms that contribute to drug resistance have been investigated, including those that are both non-mutational (presumably epigenetic) and mutational (genetic). Somatic mutations in the epidermal growth factor receptor (EGFR) gene, such as T790M mutation, deletion in exon 19, and wild-type EGFR amplification,[4] are highly correlated to favorable response to the EGFR tyrosine kinase inhibitor (EGFR-TKI) gefitinib (gef),[5] a pioneer targeted drug that has been used as the first-line treatment for patients with EGFR mutations.[6,7] Targeting gene aberrances, such as EGFR mutations, has significantly enhanced the prognosis for advanced non-small-cell lung cancer (NSCLC) patients.[7,8] Therefore, EGFR mutational status has been considered a significant biomarker and rational target for chemotherapy in advanced NSCLC patients.[5,9,10]

Accumulating evidence also suggests that microRNAs (miRNAs) play a significant role in epigenetically modulating various phenotypic changes in cancer cells.[11–15] Indeed, miRNAs may affect genetic programs through post-transcriptional silencing of target genes, either by inhibiting the translation of target mRNAs or by promoting their degradation.[16,17] These actions may lead to the regulation of numerous aspects of cancer biology, including drug resistance, epithelial-to-mesenchymal transition, and metastasis.[16–18]

Bone morphogenetic proteins (BMPs) are a family of signaling molecules that belong to the transforming growth factor β (TGF-β) superfamily.[19] Many processes, such as cell differentiation, early development, and tumor growth, are also dependent on BMP signaling.[13] Wang et al.[20] recently reported that activation of the BMP-BMP receptor (BMPR) pathway conferred resistance to EGFR-TKIs in lung cancer patients harboring EGFR mutations. We have also recently addressed the role of BMPs in cancer, and we have emphasized their function in association with miRNAs, drug resistance, and mutations.[13] Recent studies have also suggested the possibility that small-molecule BMP4 antagonists, such as LDN-193189, were able to effectively inhibit the growth of lung cancer cells and chemotherapy-resistant cancer cells.[20,21]

In the present study, we established gef-resistant NSCLC cells to investigate novel mechanisms of resistance to EGFR-TKI. In comparison with the gene expression pattern of parental NSCLC cells,

Received 1 February 2018; accepted 26 July 2018;
https://doi.org/10.1016/j.omtn.2018.07.016.

Correspondence: Hyen Joo Park, PhD, College of Pharmacy, Natural Products Research Institute, Seoul National University, Seoul 151-742, South Korea.
E-mail: phj00@snu.ac.kr
Correspondence: Sang Kook Lee, PhD, College of Pharmacy, Natural Products Research Institute, Seoul National University, Seoul 151-742, South Korea.
E-mail: sklee61@snu.ac.kr

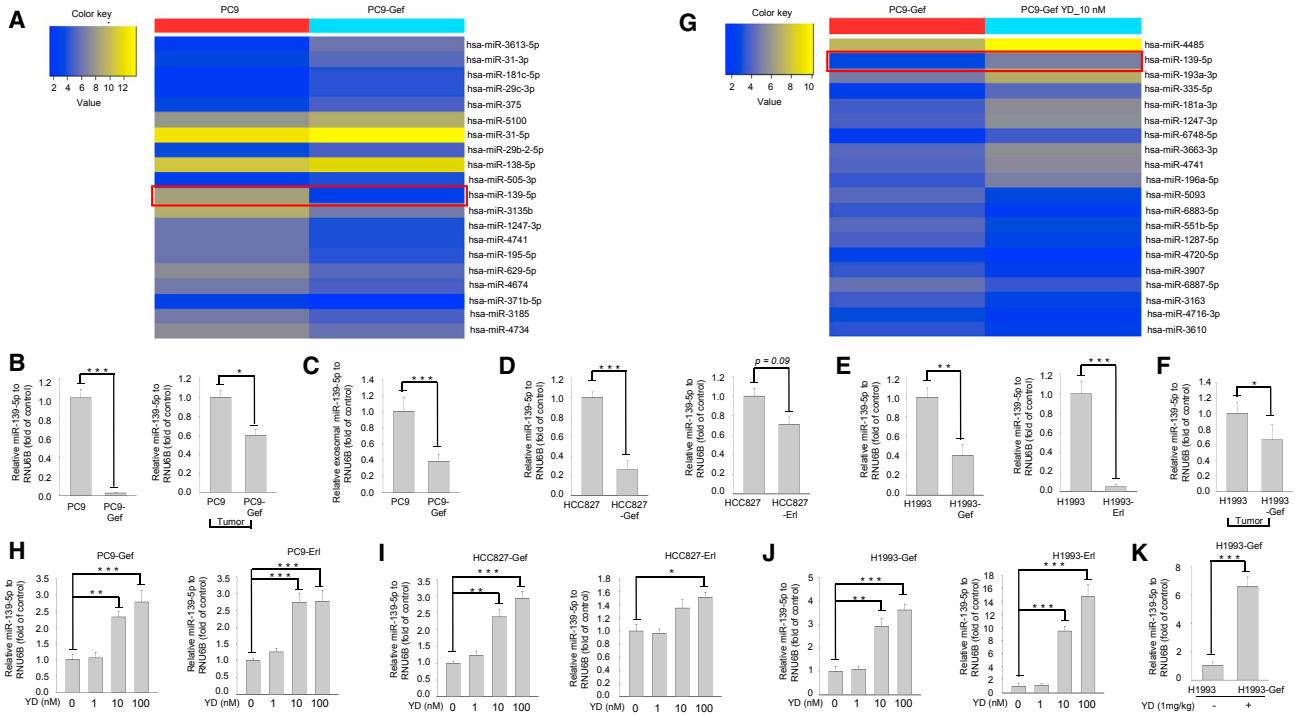

Figure 1. miR-139-5p Is a Novel miRNA Related to EGFR-TKI Resistance in NSCLC and Is Enhanced by YD

(A) Heatmap representing changes in expression of top upregulated and downregulated miRNAs in PC9-Gef cells compared to PC9 cells. (B) Characterization of PC9 cells or PC9-Gef cells (left panel) and tissues (right panel) for miR-139-5p expression. miR-139-5p levels were quantified by Taqman assay and normalized to U6 small nuclear RNA (snRNA) levels. (C) Characterization of total exosome isolation from PC9 cells and PC9-Gef cells for miR-139-5p. miR-139-5p levels were quantified by Taqman assay as described in the Materials and Methods. (D–F) Characterization of indicated cells (D and E) and tissues (F) for miR-139-5p expression. miR-139-5p levels were quantified by Taqman assay as described in the Materials and Methods. (G) Heatmap showing changes in expression of top upregulated and downregulated miRNAs in PC9-Gef cells treated with control or YD (10 nM) for 24 hr. (H–K) Effects of YD on miR-139-5p expression. (H–J) The indicated cells (H, PC9-Gef or PC9-Erl; I, HCC827-Gef or HCC827-Erl; J, H1993-Gef or H1993-Erl) were treated with YD for 24 hr, and then miR-139-5p levels were analyzed by Taqman assay as described in the Materials and Methods. (K) Relative expression of miR-139-5p in the indicated xenografts. The levels of miR-139-5p were analyzed by Taqman assay as described in the Materials and Methods. Each assay was performed in triplicate and the expression of miR-139-5p was normalized to snRNA RNU6B.

acquired gef-resistant cell lines displayed that the BMP4 gene was upregulated. We continuously attempted to elucidate the role of BMP4 in EGFR-TKI resistance in NSCLC cells and the dynamic interactions of BMP4 with the tumor microenvironment, such as miRNA or fatty acids. These findings will highlight potential new strategies for the treatment of cancer patients, especially in cases of EGFR-TKI-resistant NSCLC, by targeting BMP4.

RESULTS

miR-139-5p Is a Novel Biomarker of EGFR-TKI Resistance in EGFR-Mutant NSCLC Cells

To investigate whether miRNAs are required to establish or maintain gef resistance, we employed an miRNA array in a primary screen of EGFR-mutant NSCLC cells (PC9 cells and PC9-Gef cells). Within this array, the expression of miR-139-5p, a tumor suppressor[22,23] and a modulator of chemotherapeutic sensitivity of cancer cells,[24] was observed to be the most significantly suppressed transcript in PC9-Gef cells compared to the parental PC9 cells (Figure 1A; Table S1). We also randomly checked the expression of miR-31-5p to validate the heatmap results as an internal control, and we observed that the expression of miR-31-5p was upregulated in PC9-Gef cells versus PC9 cells (Figure S1). In addition, miR-139-5p was previously reported to be able to inhibit cell proliferation by targeting insulin-like growth factor 1 receptor (IGF1R)[25] or c-Met[26] in NSCLC cells (this was also confirmed by our group, as shown in Figure S2). Therefore, we attempted to further elucidate the role of miR-139-5p in EGFR-TKI resistance, as its function in tumorigenesis is currently unclear.

A Taqman assay confirmed that miR-139-5p was downregulated in PC9-Gef cells both *in vitro* (Figure 1B, left panel) and in tumor tissues *in vivo* (Figure 1B, right panel). In our previous review, we reported a significant relationship between exosomes and miRNAs in the drug resistance of cancer cells.[11] In the present study, we observed that the expression of exosomal miR-139-5p is also downregulated in PC9-Gef cells compared to PC9 cells (Figure 1C). Interestingly, the expression of miR-139-5p is similarly downregulated in other EGFR-TKI-resistant NSCLC cells, including HCC827-Gef cells

(EGFR mutation) versus HCC827 cells (EGFR mutation) (Figure 1D, left panel), HCC827-Erl cells versus HCC827 cells (Figure 1D, right panel), H1993-Gef cells (EGFR wild-type) versus H1993 cells (EGFR wild-type) (Figure 1E, left panel), H1993-Erl cells versus H1993 cells (Figure 1E, right panel), and H1993-Gef tumor tissues versus H1993 tumor tissues (Figure 1F).

To further identify and validate miRNAs that are specifically affected by yuanhuadine (YD), an antitumor agent,[18,27] we performed an miRNA array with PC9-Gef cells in the presence or absence of a 24-hr YD treatment. Interestingly, we found that miR-139-5p was also upregulated by YD in PC9-Gef cells (Figure 1G; Table S2). Although the expression of miR-4485 was found to be enhanced by YD treatment with approximate 2-fold changes compared to miR-139-5p expression levels in PC9-Gef cells (ratio 7.3:4.5; Table S2), the expression of miR-139-5p was found to be downregulated in PC9-Gef versus PC9 cells with approximate 28-fold changes compared to miR-4485 (ratio 50.6:1.8; Table S1). Therefore, miR-139-5p, which was mostly downregulated in gef-resistant cell lines, can be a novel biomarker in drug resistance cells, and, therefore, we primarily chose miR-139-5p as a promising candidate biomarker compared to the miR-4485. Subsequently, we further confirmed the effects of YD on miR-139-5p, and we observed that YD is able to enhance the expression of miR-139-5p not only in PC9-Gef (Figure 1H, left panel) and PC9-Erl (Figure 1H, right panel) cells but also in other drug-resistant NSCLC cells, including HCC827-Gef (Figure 1I, left panel), HCC827-Erl (Figure 1I, right panel), H1993-Gef (Figure 1J, left panel), H1993-Erl (Figure 1J, right panel), and H1993-Gef tissues *in vivo* (Figure 1K). Taken together, these findings indicated that miR-139-5p might be considered a novel biomarker associated with EGFR-TKI resistance in NSCLC cells. In addition, YD, an antitumor agent, could effectively modulate the expression of the tumor suppressor miR-139-5p in NSCLC cells with acquired resistance to EGFR-TKIs.

BMP4 Is a Candidate Biomarker in EGFR-TKI-Resistant NSCLC Cells

To identify the candidate gene markers associated with acquired resistance to EGFR-TKIs in EGFR-mutant NSCLC cells, we initially performed cDNA arrays in two different groups, as depicted in Figure 2A. BMP4 was observed to be one of the most overexpressed genes in PC9-Gef cells compared to PC9 cells. Furthermore, BMP4 was effectively suppressed by YD (Figure 2A, left panel) and miR-139-5p (Figure 2A, right panel) in PC9-Gef cells (Table 1). We further confirmed that BMP4 was upregulated in PC9-Gef cells compared to parental cells both *in vitro* (Figure 2B) and in tumor tissues *in vivo* (Figure 2C) at both the protein (upper panel) and mRNA levels (lower panel). Interestingly, we also observed that BMP4 was overexpressed in H1993-Gef (Figure 2D, left panel) and H1993-Erl cells (Figure 2D, right panel) compared to their parental cells.

Next, we transfected miR-139-5p into the resistant cells, and we observed the effects of miR-139-5p and/or YD on the expression of BMP4. When PC9-Gef, HCC827-Gef, or H1993-Gef cells were transduced with exogenous miR-139-5p, the cellular level of miR-139-5p was significantly enhanced in these indicated cells (Figure 2E). As shown in Figure 2F, transfection with miR-139-5p effectively suppressed the expression of BMP4, and co-treatment with YD enhanced this suppression. In addition, to determine whether miR-139-5p binds directly to BMP4 mRNA, we performed ribonucleoprotein immunoprecipitation (RIP) assay to pull down miRNAs associated with RNA-induced silencing complex (RISC). An anti-AGO2 antibody was used to isolate miRNAs and mRNAs that were incorporated in RISC. In H1993-Gef cells that were stably overexpressing miR-139-5p, BMP4 mRNA was enriched in RISC as compared with the immunoglobulin G (IgG) control (Figure 2G). Anti-AGO-2 antibody also significantly enriched miR-139-5p, as detected by Taqman PCR, compared with a negative control (NC) mimic in PC9-Gef and H1993-Gef cells (Figure 2H), indicating that miR-139-5p directly interacts with BMP4 mRNA. The expression of BMP4 was also effectively suppressed by YD in *in vivo* tumor tissues analyzed by real-time PCR (Figure 2I, upper panel), immunoblotting (Figure 2I, lower panel), and immunohistochemistry (IHC) (Figure 2J).

Taken together, these data suggest that BMP4 is a novel marker associated with acquired EGFR-TKI resistance in EGFR-mutant NSCLC cells and that BMP4 expression can be effectively suppressed by miR-139-5p and/or YD treatment to overcome resistance in these cells.

BMP4 Affects the Growth of EGFR-TKI-Resistant NSCLC Cells

The critical function of BMPs in cancer is still unclear, as discussed in a recent review by our group.[13] However, in human NSCLC, blockage of BMP signaling is considered an effective therapeutic approach for lung cancer patients.[28] Kim et al.[29] recently reported that BMP4 depletion might suppress tumorigenesis and metastasis in lung adenocarcinoma cells. Furthermore, the growth and metastasis of lung adenocarcinoma were potentiated by BMP4-mediated immunosuppression.[30] Therefore, we determined whether the knockdown of BMP4 by small interfering RNA (siRNA) affects the growth of the EGFR-TKI-resistant NSCLC cells.

We first measured the knockdown efficiency of various siBMP4s, and we selected specific siRNAs for further study in the resistant cells (Figures 3A and 3B). As depicted in Figure 3C, knockdown of BMP4 enhanced the growth-inhibitory activity of gef in PC9-Gef and H1993-Gef cells (Figure 3C). In addition, the knockdown of BMP4 also significantly suppressed colony formation in PC9-Gef and H1993-Gef cells (Figure 3D). Similarly, knockdown of BMP4 also inhibited cell invasion (Figure 3E) and migration (Figure 3F) in PC9-Gef cells. The *in vivo* effects of BMP4 on tumor growth were subsequently investigated in BALB/c nude mouse xenograft models implanted with gef-resistant NSCLC cells. The gef-resistant cells were initially established as stable BMP4-knockout cells. As shown in Figures 3G and 3H, shBMP4-A and shBMP4-D were the most efficient in knocking down BMP4 expression in PC9-Gef and H1993-Gef cells compared to shBMP4-B and shBMP4-C. Mice were then subcutaneously injected in the right axilla with empty vector-transfected

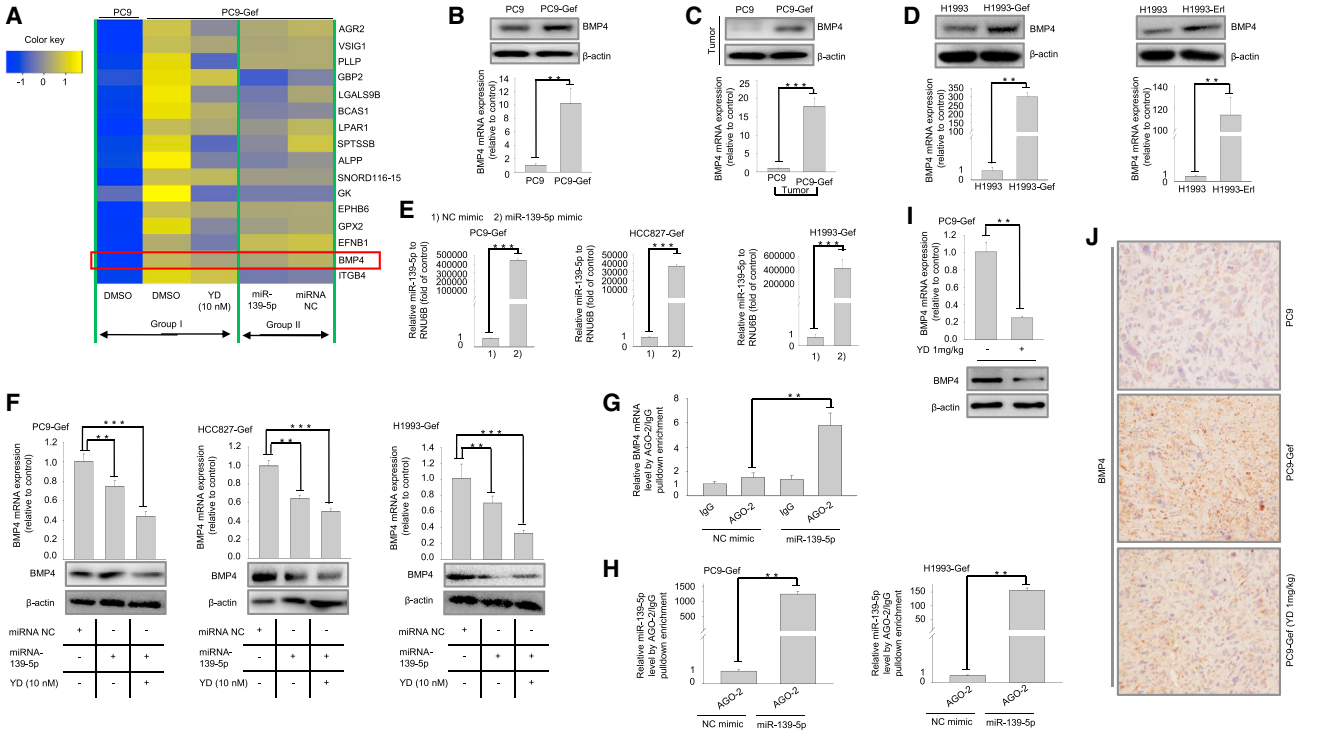

Figure 2. BMP4 Is Identified by Combining Target Arrays

(A) Heatmap showing relative expression among all groups. Left panel: PC9-Gef cells were treated for 24 hr with 10 nM YD or vehicle control. Right panel: PC9-Gef cells were transfected with miR-139-5p or miRNA mimic for 48 hr. Rows represent genes and columns represent samples. Yellow blocks represent high expression and blue blocks low expression relative to control cells. (B–D) Characterization of the indicated parental or drug-resistant cell lines and tissues (PC9 and PC9-Gef cells (B) or tissues (C); H1993 and H1993-Gef cells (D, left panel) and tissues (D, right panel) for BMP4 expression at both the protein and mRNA levels. (E) Effects of miR-139-5p mimic on miR-139-5p expression in the indicated gef-resistant cell lines. The indicated gef-resistant cell lines were cultured in 6-well plates and then transfected with negative control mimic or miR-139-5p for 48 hr (50 pmol/well). The expression levels of miR-139-5p were determined by Taqman assay with specific primers for mature miR-139-5p. Expression levels in each sample were normalized to levels of U6 snRNA. (F) The indicated cells were post-transfected with miR-139-5p for 24 hr. Then, the indicated cells were further treated with YD (10 nM) for 24 hr. The cell lysates were subsequently analyzed by real-time PCR and immunoblotting, as described in the Materials and Methods. (G and H) RIP assay of miR-139-5p interaction with BMP4 mRNA. Co-immunoprecipitated BMP4 mRNA (G) and miR-139-5p (H) by anti-AGO-2 RIP are shown. The data were normalized to β-actin or U6 snRNA, respectively. NC, negative control. (I) Relative expression of BMP4 in the indicated xenograft tumors. The levels of BMP4 were analyzed by real-time PCR (upper panel) or immunoblotting (lower panel), as described in the Materials and Methods. (J) Immunohistochemical analysis for BMP4 in the indicated tumor tissue sections.

PC9-Gef cells and H1993-Gef cells or stable BMP4-A- or BMP4-D-knockout PC9-Gef and H1993-Gef cells. At 40 days (PC9-Gef) and 30 days (H1993-Gef) after inoculation, the mice were sacrificed, and the tumors in each mouse were excised and photographed. As shown in Figures 3I and 3J, the tumors in the stable BMP4-knockout group were smaller than those in the vector-treated groups, demonstrating that BMP4 is able to enhance the growth of gef-resistant NSCLC cells.

Suppression of BMP Signaling Inhibits the Growth of EGFR-TKI-Resistant NSCLC Cells

Fotinos et al.[31] recently reported that the suppression of BMP signaling is a valid therapeutic strategy in lung cancer and that the dorsomorphin derivative LDN-193189, a BMP type I receptor inhibitor, had significant growth-inhibitory activity against NSCLC cells compared to non-transformed cells. Our findings in this study confirm that BMP4 is one of the principal paracrine factors that stimulate the growth of drug-resistant cancer cells. To further confirm whether knockdown of the BMP-BMPR pathway may suppress the growth of drug-resistant cancer cells, the efficacy of LDN-193189 was investigated in tumor growth. LDN-193189 effectively inhibits the growth of cancer cells (Figure 4A); this effect was in part associated with the suppression of Smad1/5 activation (p-Smad1/5) in the resistant cancer cells (Figure 4B). We further investigated the possible therapeutic approach using a combination of LDN-193189 and YD, an antitumor agent, in drug-resistant cancer treatment. As shown in Figure 4C, the combination of LDN-193189 and YD enhanced growth inhibition in cancer cells compared to treatment with LDN-193189 alone. Notably, LDN-193189 also effectively suppressed tumor growth in nude mice bearing gef-resistant NSCLC cells *in vivo* (Figures 4D and 4E), without any significant change in body weight (Figure 4F). The analysis of tumor tissues also revealed suppressed

Table 1. Top Genes that Were Upregulated in PC9-Gef Cells versus PC9 Cells and Also Affected by YD 10 nM and miR-139-5p in PC9-Gef Cells

No.	Gene_Symbol	Gene Accession No.	Gene Description	PC9 versus PC9-Gef	PC9-Gef YD 10 nM versus PC9-Gef	PC9-Gef miR-139-5p versus PC9-Gef miR-CTL (30 hr)
1	BMP4	NM_001202	bone morphogenetic protein 4	−11.89	−1.48	−1.28
2	SNORD116-155	NR_003330	small nucleolar RNA, C/D box 116-15	−9.45	−1.13	−1.02
3	AGR2	NM_006408	anterior gradient 2, protein disulphide isomerase family member	−9.45	−2.33	−1.20
4	VSIG1	NM_001170553	V-set and immunoglobulin domain containing 1	−4.77	−1.29	−1.06
5	PLLP	NM_015993	plasmolipin	−4.77	−3.14	−1.01
6	BCAS1	NM_001316361	breast carcinoma amplified sequence 1	−4.59	−1.59	−1.07
7	ALPP	NM_001632	alkaline phosphatase, placental	−3.80	−2.47	−1.14
8	EPHB6	NM_001280794	EPH receptor B6	−3.79	−1.23	−1.01
9	LPAR1	NM_001401	lysophosphatidic acid receptor 1	−3.61	−1.21	−1.33
10	GBP2	NM_004120	guanylate-binding protein 2, interferon inducible	−3.53	−1.29	−1.40
11	EFNB1	NM_004429	ephrin-B1	−2.82	−1.49	−1.07
12	LGALS9B	NM_001042685	lectin, galactoside binding, soluble, 9B	−2.72	−1.74	−1.3
13	SPTSSB	NM_001040100	serine palmitoyltransferase, small subunit B	−2.57	−2.02	−1.47
14	ITGB4	NM_000213	integrin beta 4	−2.56	−1.13	−1.04
15	GK	NM_000167	glycerol kinase	−2.52	−2.50	−1.01
16	GPX2	NM_002083	glutathione peroxidase 2	−2.48	−1.56	−1.05

expression of the cell proliferation biomarker Ki-67 (Figure 4G), as confirmed by consistent findings in *in vitro* cell culture systems. These data suggest that the suppression of endogenous BMP signaling may represent a possible strategy for the treatment of drug-resistant NSCLC cells.

BMP4 Affects Cancer Cell Metabolism via the Modulation of ACSL4 and p53

To further investigate the downstream targets of BMP4 and its functional activity in cancer cells, a cDNA microarray was performed on BMP4-depleted EGFR-TKI-resistant NSCLC cells. Genes associated with cell metabolism were the genes most affected by BMP4 depletion (Figure 5A; Table S3). Among these genes, Acyl-CoA synthetase long-chain family member 4 (ACSL4) was highly suppressed in PC9-Gef cells (Figure 5B; Table S4). Previous studies suggested that ACSL enzymatic activity plays a significant role in the maintenance of mutant lung cancer; furthermore, fatty acid oxidation mediated by ACSL enzymes is required for mutant lung tumorigenesis.[32,33] In this study, we found that knockdown of ACSL4 inhibits PC9-Gef colony formation (Figure S3). In addition, BMP4 depletion suppressed ACSL4 expression at both the mRNA (Figure 5C, upper panels) and protein levels (Figure 5C, lower panels). However, ACSL4 knockdown did not affect BMP4 expression at both the mRNA (Figure S4) and protein levels (Figure 5D, lower panels). These data indicate that ACSL4 seems to be one of the downstream target proteins mediated by BMP4.

Interestingly, ACSL4 is considered an important enzyme in energy metabolism,[34–36] and BMP4 is also associated with oxidative metabolism in cells,[37–39] as depicted in Figure 5E. Therefore, we determined whether the effects of BMP4 on the production of main energy metabolites were catalyzed by ACSL4. We found that BMP4 depletion suppressed the enzymatic activity of ACSL4 and thus restored metabolites, including fatty acids (-CH_3), triglycerides, and cholesterol esters, in the resistant cells (Figure 5F). We also found that BMP4 depletion stimulated p-p53 expression, as shown by phosphor-kinase array (Figure 5G). This upregulation of p-p53 (Ser15) was confirmed by western blot analysis (Figure 5H) in PC9-Gef cells. Recent findings suggest that the tumor suppressor p53 is also related to the regulation of lipid metabolism, including enhancing fatty acid oxidation and suppressing fatty acid synthesis.[40,41] Therefore, the activation of p53 expression by BMP4 depletion might affect lipid metabolism catalyzed by ACSL4. Taken together, BMP4 seems to be associated with cancer cell metabolism through the regulation of ACSL4 and the tumor suppressor p53.

DISCUSSION

Recent studies revealed that miRNAs might be applicable as potential biomarkers to predict responses to chemotherapy and survival of patients with malignant tumors.[11] Indeed, downregulation of miR-139-5p was observed in colorectal cancer,[23] hepatocellular carcinoma (HCC),[42] and NSCLC.[26] BMP4 genetic variants and protein expression are also highly associated with platinum-based chemotherapy response and prognosis in NSCLC.[43] NSCLC patients with high BMP4 expression were more likely to be resistant to chemotherapy than those with low BMP4 expression.[43] Recent studies using integrated epigenomics also identified BMP4 as a modulator of cisplatin sensitivity in gastric cancer (GC), and they indicated that

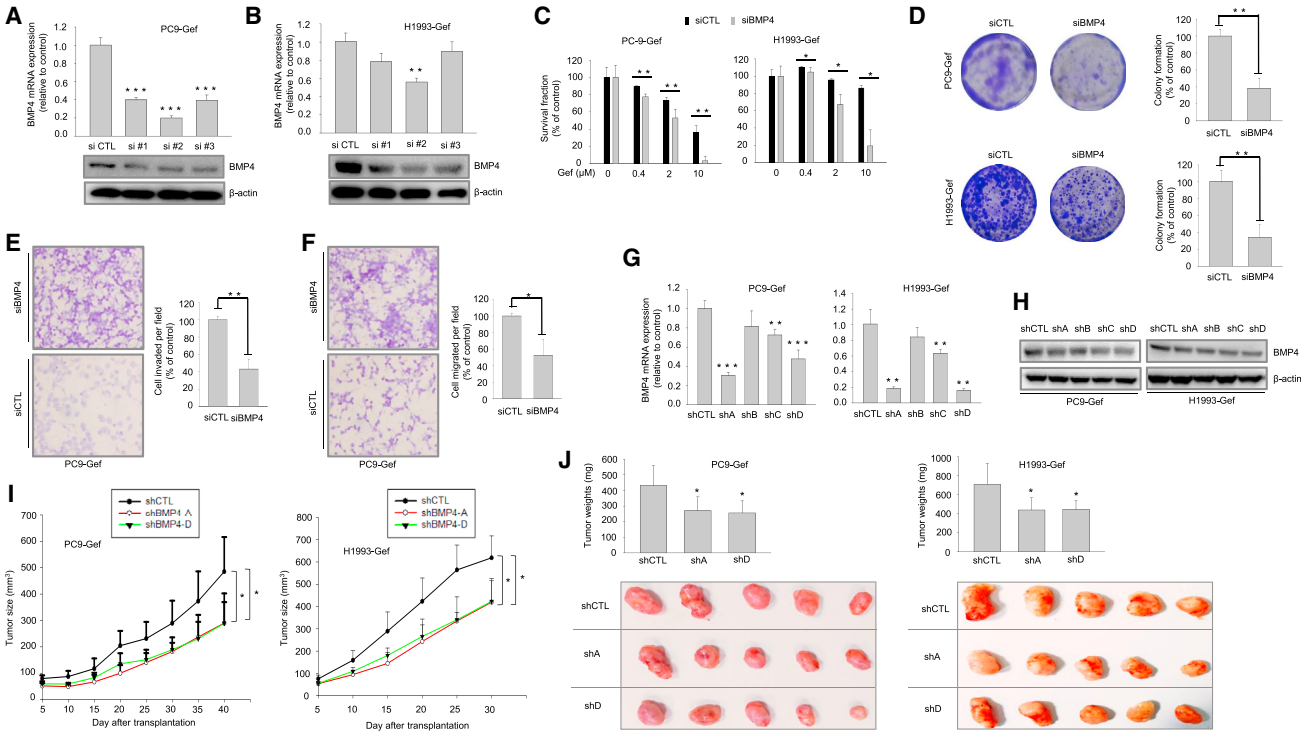

Figure 3. BMP4 Depletion Modulates the Growth of EGFR-TKI-Resistant NSCLC Cells

(A and B) Confirmation of BMP4-knockdown efficiency at the mRNA (upper panels) and protein levels (lower panels) in PC9-Gef (A) and H1993-Gef (B) cells. (C) Cells were transiently post-transfected with control or BMP4 #2 siRNA for 48 hr, and then incubated with the indicated concentrations of gef. Cell viability was further assessed by SRB assay as described in the Materials and Methods. (D) The indicated cells were transiently post-transfected with either scramble siRNA or BMP4 #2 siRNA for 48 hr, then cultured for colony formation assays as described in the Materials and Methods. (E and F) PC9-Gef cells were transiently post-transfected with either scramble siRNA or BMP4 #2 siRNA for 48 hr, then cultured for invasion (E) and migration (F) assays as described in the Materials and Methods. (G and H) Confirmation of BMP4-knockdown efficiency by shRNA at both the mRNA (G) and protein (H) levels in stable knockout PC9-Gef and H1993-Gef cells, as described in the Materials and Methods. (I and J) Tumor-forming ability of BMP4-silenced gef-resistant NSCLC cells. BALB/c nude mice received subcutaneous transplants of PC9-Gef-sh control (n = 5) and PC9-Gef-shBMP4 (shA or shD) (n = 5) cells or H1993-Gef-sh control (n = 5) and H1993-Gef-shBMP4 (shA or shD) (n = 5) cells. (I) Tumor volumes at the indicated time points. (J) Tumor weights (upper panels) and representative photographs 40 days (PC9-Gef) and 30 days (H1993-Gef) after injection (lower panels).

its expression status may elicit promising biomarkers for cisplatin-resistant GC.[44,45] In colorectal cancer, however, BMP4 can stimulate terminal differentiation and increase the response to chemotherapy in chemo-resistant colorectal cancer stem cells (CRC-SCs).[46]

In the present study, we found that the expression of miR-139-5p is significantly downregulated in gef-resistant NSCLC cells compared to parental cells, suggesting that dysregulation of miR-139-5p is involved in the development of drug-resistant lung cancer. The function of miR-139-5p in the resistant cancer cells was confirmed by employing the antitumor agent YD to effectively upregulate the expression of miR-139-5p in gef-resistant NSCLC cells. Further studies were designed to identify the putative role of miR-139-5p in gef-resistant cancer cells. The combination of cDNA profile arrays and miRNA arrays, with YD-induced restoration of miR-139-5p, led to the novel identification of BMP4 as one of the most overexpressed genes in gef-resistant NSCLC cells. These findings suggest that there is an inverse correlation between the expression of miR-139-5p and BMP4 levels in EGFR-TKI-resistant NSCLC cells. Therefore, the modulation of either miR-139-5p or BMP4 might be a novel strategy to overcome EGFR-TKI resistance in EGFR-mutant NSCLC cells.

Indeed, we demonstrated the pro-tumorigenic role of BMP4 through knockdown of BMP4 in gef-resistant NSCLC cells. We also revealed that BMP4 regulates ACSL4 to affect lipid metabolism. The upregulation of BMP4 and ACSL4 leads to higher energy metabolism in resistant cancer cells, enabling cancer cells to enhance cell growth and acquire drug resistance. Additionally, the relationship between BMP4 and energy metabolism was also confirmed by the enhanced expression of p53 in BMP4-depleted EGFR-mutant gef-resistant NSCLC cells (PC9-Gef). Recent findings suggest that activation of the BMP-BMPR pathway may confer resistance to EGFR-TKIs in lung cancer patients with EGFR mutations.[20] Subsequently, targeting the BMP pathway with various BMP inhibitors could provide a potential therapy for cancer treatment. In this vein, the dorsomorphin derivative LDN-193189 was reported to significantly suppress the proliferation of NSCLC cells, but not non-transformed cells.[31] LDN-193189 was also effective against chemotherapy-resistant epithelial ovarian cancer

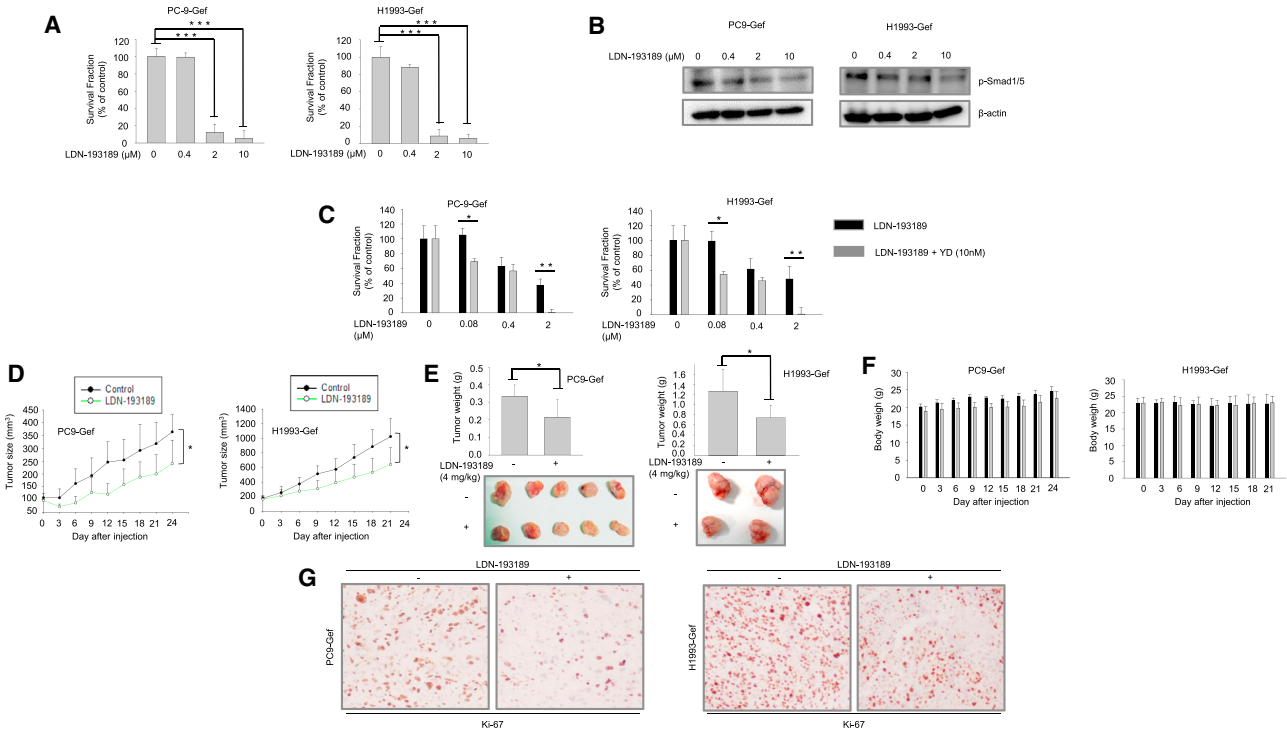

Figure 4. LDN-193189 Treatment Attenuates EGFR Mutation Resistance in *In Vivo* Tumor Growth

(A) The indicated cells were treated with LDN-193189 for 72 hr and cell proliferation was determined by SRB assay. The IC_{50} values were calculated using the TableCurve 2D software and the data are presented as the mean ± SD. (B) PC9-Gef cells and H1993-Gef cells were treated with the indicated concentrations of LDN-193189 for 24 hr, and the cell lysates were further analyzed by immunoblotting using β-actin as a loading control. (C) PC9-Gef cells and H1993-Gef cells were treated with the indicated concentrations of LDN-193189 either alone or in combination with 10 nM YD for 48 hr. Cell proliferation was determined by SRB assay. (D) PC9-Gef cells (6×10^6 cells/mouse) and H1993-Gef cells (5×10^6 cells/mouse) were implanted subcutaneously into the flanks of BALB/c-nude mice. 3 weeks of dosing with LDN (4 mg/kg body weight for PC9-Gef cells or 5 mg/kg body weight for H1993-Gef cells) was initiated when the PC9-Gef tumor volumes reached approximately 100 mm^3 and H1993-Gef tumor sizes reached approximately 170 mm^3. The tumor volumes were measured every 3 days (n = 5 mice per group). The error bars represent the means ± SD. (E) Tumors were excised from animals on days 4 (PC9-Gef) or 21 (H1993-Gef) after treatment and tumor weights were measured. (F) Body weights of the mice were monitored during the experiments for toxicity. (G) Immunohistochemical analysis of PC9-Gef and H1993-Gef xenograft tumors. Formalin-fixed, paraffin-embedded tumor sections were blocked and probed with an antibody against Ki-67, which was detected using the LSAB + System-HRP kit (Dako).

cells,[21] and it enhanced the chemo-sensitivity of Smad4-silenced colorectal cancer cells.[47] Based on these studies, we attempted to determine whether LDN-193189 is able to suppress gef-resistant NSCLC tumor growth *in vivo*. LDN-193189 effectively suppressed tumor growth in nude mice bearing gef-resistant NSCLC cells.

In conclusion, BMP4 overexpression is partially associated with gef resistance in NSCLC cells, and BMP4 can be suppressed by miR-139-5p and YD. BMP4 also interacts with ACSL4 and the p53-signaling pathway, both of which are highly connected to lipid energy metabolism in cancer cells. These findings suggest that BMP4 may be considered a potential prognostic biomarker or therapeutic target for patients with gef-resistant NSCLC.

MATERIALS AND METHODS

Cancer Cell Lines and Reagents

H1993 human lung carcinoma cells were obtained from the American Type Culture Collection (Manassas, VA, USA). gef-resistant cells were developed as previously described[27] and all cells were cultured as previously described.[27,48] In brief, gef-resistant H1993 and erlotinib (erl)-resistant H1993 cells were developed from the parental H1993 cells through continuous exposure to gradually increasing drug dosages up to 10 μM each of gef and erl. Subsequently, resistant H1993 cells were maintained in medium containing 10 μM gef or erl. LDN-193189 was purchased from Selleckchem (Houston, TX, USA).

Establishing Stable Cell Lines

Murine BMP4 small hairpin RNAs (shRNAs) (EZWC0CL102, TF306390A, CCN 185819-A; EZWB0CL101, TF306390B, CCN 185818-B; EZWA0CL101, TF306390C, CCN 185817-C; and EZVZ0CL101, TF306390D, CCN 185816-D) and control shRNA (TR30015, lot 0116) were purchased from OriGene (Rockville, MD, USA) and introduced into the indicated cells by viral infection. Stable cell lines were established following greater than 2 weeks of antibiotic selection, according to the manufacturer's instructions.

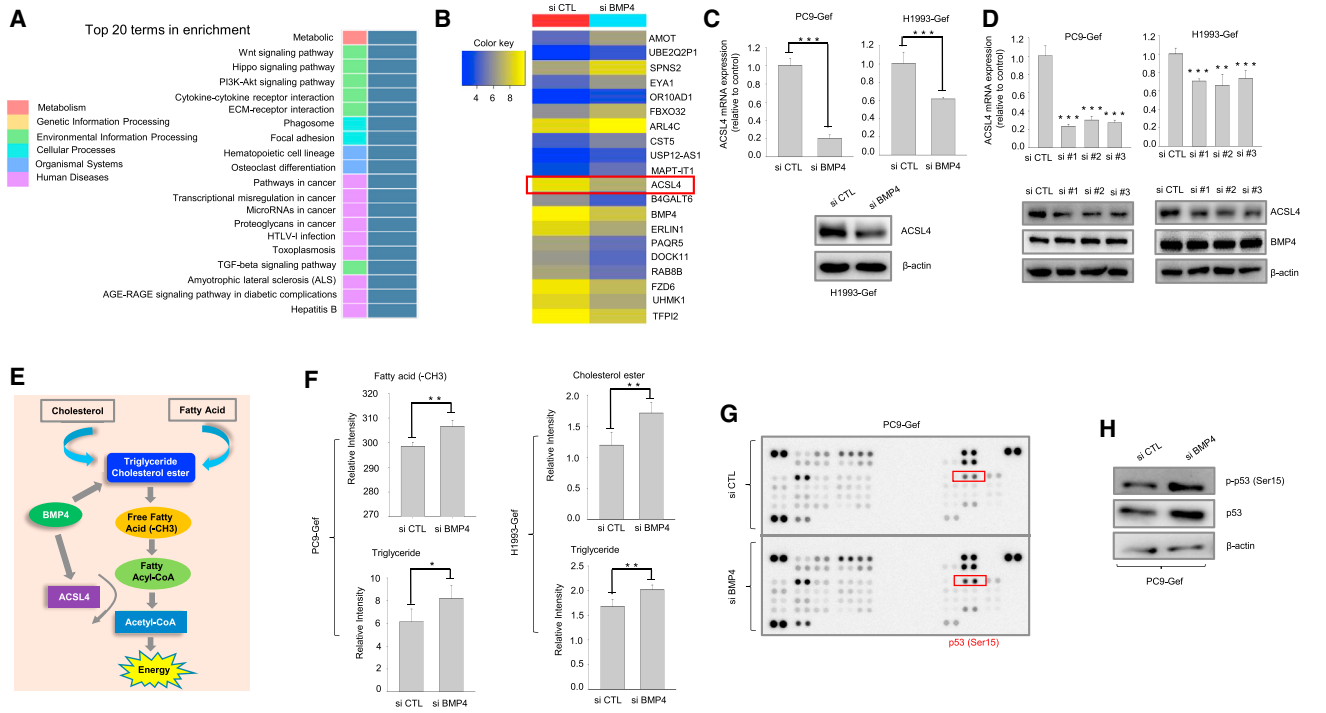

Figure 5. BMP4 Knockdown Influences Metabolism and p53

(A) Heatmap showing and comparing top enriched terms. Enrichment test based on the gene ontology (GO, http://geneontology.org/) database was conducted using the significant gene list. Significant enrichments are displayed in blue (p value = 0.0001). (B) Heatmap representing changes in expression of top upregulated and downregulated genes in PC9-Gef cells transfected with control or BMP4 #2 siRNA. (C) PC9-Gef and H1993-Gef cells were transfected with control or BMP4 siRNA for 48 hr, then cell lysates were subjected to real-time PCR (top panels) or immunoblotting (bottom panels). (D) PC9-Gef and H1993-Gef cells were transfected with control or ACSL4 siRNA for 48 hr, then cell lysates were subjected to real-time PCR (top panels) or immunoblotting (bottom panels). (E) Schematic diagram illustrating the proposed BMP4 pathway modulating energy metabolism through ACSL4 and triglycerides. (F) PC9-Gef and H1993-Gef cells were transfected with control and BMP4 #2 siRNA for 48 hr, and then cell lysates were further processed for metabolic analyses as described in the Materials and Methods. (G) PC9-Gef cells were transfected with control or siBMP4 #2 siRNA for 48 hr, and cell lysates were subjected to the phosphor-kinase array. p-p53 (Ser15) expression levels are indicated. (H) Indicated cells were transfected with either siBMP4 #2 or siCTL for 48 hr, and then lysates were analyzed for p-p53 and total p53 by immunoblotting.

Microarray Expression Analysis

RNA Quality Check

RNA purity and integrity were evaluated using the ND-1000 Spectrophotometer (NanoDrop, Wilmington, DE, USA) and the Agilent 2100 Bioanalyzer (Agilent Technologies, Palo Alto, CA, USA).

Affymetrix Whole-Transcript Expression Arrays

The Affymetrix whole-transcript expression array procedure was executed according to the manufacturer's protocol (GeneChip Whole Transcript PLUS reagent kit). cDNA was synthesized using the GeneChip WT (whole-transcript) Amplification kit, as described by the manufacturer.

The sense cDNA was then fragmented and biotin labeled with TdT (terminal deoxynucleotidyl transferase) using the GeneChip WT Terminal labeling kit.

Approximately 5.5 μg labeled DNA target was hybridized to the Affymetrix GeneChip Human 2.0 ST Array for 16 hr at 45°C. Hybridized arrays were washed and stained on a GeneChip Fluidics Station 450 and scanned on a GCS3000 Scanner (Affymetrix). Signal values were computed using the Affymetrix GeneChip Command Console software.

Raw Data Preparation and Statistical Analysis

Raw data were extracted automatically as part of the Affymetrix data extraction protocol using the Affymetrix GeneChip Command Console software (AGCC). After importing CEL files, the data were summarized and normalized using the robust multi-average (RMA) method within the Affymetrix Expression Console software (EC). We exported results with gene-level RMA analysis and performed differentially expressed gene (DEG) analysis. Fold changes were used to determine statistical significance of the expression data. For each DEG set, hierarchical cluster analysis was performed using complete linkage and Euclidean distance as measures of similarity. Gene enrichment and functional annotation analysis of the list of significant genes was performed using gene ontology (http://www.geneontology.org/) and Kyoto Encyclopedia of Genes and Genomes (KEGG) (https://www.genome.jp/kegg/). All data analysis and visualization of DEGs were conducted using R 3.1.2 (www.r-project.org).

Xenograft Studies

All procedures involving animals (BALB/c nude mice, 4–6 weeks old) were reviewed and approved by Seoul National University (permission SNU-161117-1).

For tumorigenicity assays in nude mice, the indicated cells were subcutaneously injected into the right axilla of BALB/c nude mice (n = 5) in a total volume of 200 μL culture medium (5×10^6 cells). At 40 days (PC9-Gef) and 30 days (H1993-Gef) after inoculation, the mice were humanely killed and the tumors were excised and photographed.

For drug response assays, the indicated cells (5×10^6 cells in 200 μL medium) were injected subcutaneously into the flanks of nude mice and tumors were allowed to grow. When the tumor volume reached approximately 100 mm^3 (PC9-Gef) or 160 mm^3 (H1993-Gef), the mice were randomized into vehicle control and treatment groups (n = 5). Then, these mice were treated with vehicle or LDN-193189 (4 mg/kg for PC9-Gef, 5 mg/kg for H1993-Gef) for 3 weeks (5 days on, 2 days off). Tumor volumes were determined using digital calipers using the formula $(L \times W \times M \times \pi)/6$ as described previously.[27] The body weight of each mouse was also monitored for toxicity analyses.

Phospho-antibody Array Analysis

Phospho-antibody array analysis was performed using the Proteome Profiler Kit ARY003B (R&D Systems) according to the manufacturer's instructions. Briefly, cells were transfected with siBMP4 for 48 hr. Cells were then lysed and centrifuged at 14,000 × *g* for 10 min. 500 μg cellular extract was then subjected to a protein array. Phosphorylated kinases were identified by incubating arrays with biotinylated detection antibodies, streptavidin-horseradish peroxidase (HRP) antibodies, and chemiluminescent detection reagents.

Metabolic Analysis

Metabolite Extraction

Metabolites were extracted from cells in 600 μL chilled methanol-chloroform mixture (2:1). This mixture was vortexed for 30 s, frozen on liquid nitrogen for 2 min, and thawed at room temperature for 1.5 min; this process was repeated three times. Then, 200 μL chilled chloroform and 200 μL chilled water were added and the mixture was vigorously vortexed and then centrifuged at 15,000 × *g* for 20 min at 4°C. The upper aqueous phase and lower organic solvent phase were collected separately and dried with a centrifugal evaporator (Vision). The residuals were stored at −20°C until analysis.

NMR Experiments and Statistical Analysis

For lipid analyses, the organic layer samples were dissolved in 500 μL deuterated chloroform and transferred into a 5-mm nuclear magnetic resonance (NMR) tube. The heteronuclear single quantum coherence (HSQC) NMR spectra were obtained using 800 MHz Bruker Avance spectrometers equipped with a cryogenic triple-resonance probe at the College of Pharmacy, Seoul National University (Seoul, South Korea). 2D HSQC spectra were processed and analyzed with NMRView J software (One Moon Scientific) to extract quantitative information as follows: the integrated peak area of the 2D HSQC spectra was normalized against the total peak area and then used for statistical analyses. Metabolite identification was performed using in-house and public databases.[49]

Exosome Isolation

Total exosomes were extracted with Invitrogen Total Exosome Isolation Reagent (catalog number 4478359, publication: MAN0006949) from Invitrogen (Thermo Fisher Scientific), according to the manufacturer's instructions.

Immunoblot Analysis

Western blot analysis was performed as described previously, using equal amounts of protein from each cell lysate.[48,50–52] The following antibodies were used: anti-BMP4 (ab39973, Abcam, UK); anti-p53 (DO-1) (sc-126); anti-β-actin (C4) (sc-47778) (Santa Cruz Biotechnology, Santa Cruz, CA, USA); anti-p-Smad1/5 (Ser463/465) (9516); anti-p-p53 (Ser15) (9284) (Cell Signaling Technology, Danvers, MA, USA); and anti-ACSL4 (PA5-27137) (Invitrogen, CA, USA).

Sulforhodamine B Assay

PC9-Gef cells and H1993-Gef cells were post-transfected with control or BMP4 siRNA for 48 hr, and then the indicated cells (1×10^4 cells/mL) were seeded in 96-well plates with the indicated concentrations of gef and further analyzed as previously described.[48] Similarly, PC9-Gef cells were also post-transfected with miRNA mimic or miR-139-5p for 48 hr, and then the transfected cells were further analyzed as previously described.[48]

Combinatorial Drug Analysis

The indicated cells were plated in 96-well culture plates and then exposed to various concentrations of LDN-193189 and YD (10 nM) at a 1:1 ratio. After 48 hr of incubation, cell proliferation was evaluated using the sulforhodamine B (SRB) assay, as previously described.[48]

Real-Time PCR

Total cell or tumor tissue RNA was extracted with TRI reagent (Invitrogen, Grand Island, NY, USA), and then RT-PCR analysis was carried out as described previously.[48,50] Gene-specific primers for real-time PCR were synthesized by Bioneer (Daejeon, Korea): human ACSL4 sense, 5′-TTCATCTCTTGGACTTTGCTCA-3′; antisense, 5′-TGTACTGTACTGAAGCCCACACTT-3′; human BMP4 sense, 5′-GGGATGTTCTCCAGATGTTCTT-3′; and antisense, 5′-TCCA CAGCACTGGTCTTGAG-3′.

Transfection of siRNAs and miRNAs

The siRNAs targeting BMP4 (siBMP4-1, 1012726; siBMP4-2, 1012728; and siBMP4-3, 1012733) and ACSL4 (siACSL4-1, 1001674; siACSL4-2, 1001681; and siACSL4-3, 1001676), as well as the negative control siRNA (catalog number SN-1002), miR-139-5p mimic (mature sequence 5′-UCUACAGUGCACGUGUCUCC AGU-3′), and miRNA mimic negative control (catalog number SMC-2002), were synthesized by Bioneer (Daejeon, Korea), and

they were transfected into the cell lines by electroporation using Lipofectamine RNAiMAX (Invitrogen, Carlsbad, CA, USA), according to the manufacturer's recommendations. The cells were post-transfected within the indicated times and harvested for further analysis.

Colony Formation Assay

The indicated cells were seeded in 24-well plates at a density of 200 cells per well. Following an overnight incubation of seeded plates, the indicated cells were transfected with the indicated siRNA or siRNA control for 48 hr, and they were then further analyzed by colony formation assay, as described previously.[18]

Cell Migration and Invasion Assays

Cell invasion assays were performed in 24-well Transwell plates with polycarbonate (polyvinylidene fluoride [PVDF]) filters (8-mm pore size, Corning, USA), while changes in cell migration were analyzed using Transwell assays without the incorporation of Matrigel. The indicated cells were post-transfected with siBMP4 or siRNA control, and they were then further analyzed using cell migration and invasion assays, as described previously.[18]

Taqman miRNA Assay

To determine the expression of miRNAs in human cancer cells, we used the TaqMan MiRNA Assay kit (Applied Biosystems) (catalog number 4427975) according to the manufacturer's protocol. The mature miR-139-5p sequence was as follows: 5′-UCUACAGU GCACGUGUCUCCAG-3′ (catalog number 4427975, assay ID 002289, assay type Taqman miRNA assay). The mature miR-31-5p sequence was as follows: 5′-AGGCAAGAUGCUGGCAUAGCU-3′ (catalog number 4427975, assay ID 002279, assay type Taqman miRNA assay). All reactions were performed in triplicate.

Ex Vivo Biochemical Analysis of Tumors

A portion of the frozen tumor excised from each nude mouse was thawed on ice and homogenized using a hand-held homogenizer in Complete Lysis Buffer (Active Motif, Carlsbad, CA, USA), as described previously.[18] The protein concentrations of the tumor lysates were calculated and aliquots were stored at −80°C.

Immunohistochemistry

Immunohistochemical analysis of tumors was carried out as described previously, using the indicated antibodies.[18]

RIP Assay

The RIP-Assay kit for miRNA (MBL) was employed to confirm between miR-139-5p and BMP4 interaction following the manufacturer's instructions. Briefly, fresh cellular extracts from PC9-Gef cells or H1993-Gef cells (10^6) were co-immunoprecipitated with 20 μg RIP-certified anti-EIF2C2/AGO2 mouse monoclonal antibody (MBL) overnight at 4°C, one of the RISC protein components, previously conjugated with Sepharose Protein G beads (Amersham Biosciences, GE Healthcare). Rabbit IgG was used as negative control. BMP4 and miR-139-5p expression levels were evaluated after total RNA isolation from antibody-immobilized Protein G agarose bead-ribonucleoprotein (RNP) complexes by real-time PCR (as described in the Materials and Methods). Data were normalized to control samples from three independent experiments.

Statistical Analysis

The data are presented as the mean ± SD for the indicated number of independently performed experiments. Statistical significance (*$p < 0.05$, **$p < 0.01$, ***$p < 0.001$, or ns [not significant]) was assessed using Student's t test. All statistical tests were two sided.

SUPPLEMENTAL INFORMATION

Supplemental Information includes four figures and four tables and can be found with this article online at https://doi.org/10.1016/j.omtn.2018.07.016.

AUTHOR CONTRIBUTIONS

D.-H.B. designed and performed most of the experiments, assisted by T.-T.-T.L. and D.K. H.J.P. discussed the results and contributed to the manuscript. Y.J.A. and S.P. performed metabolic analyses. D.-H.B. wrote the initial draft of the manuscript. S.K.L. designed and supervised the experiments and edited the manuscript.

CONFLICTS OF INTEREST

The authors declare no conflict of interest.

ACKNOWLEDGMENTS

We thank Jin Kyung Rho (Department of Pulmonology and Critical Care Medicine; Asan Institute for Life Sciences, Daejeon, South Korea) for generously providing the HCC827, HCC827-Gef, HCC827-Erl, PC9, PC9-Gef, and PC9-Erl cell lines. This study was funded by the Basic Science Research Program through the National Research Foundation of Korea (NRF), which is funded by the Ministry of Education (2015R1D1A1A02062012).

REFERENCES

1. Diaz, L.A., Jr., Williams, R.T., Wu, J., Kinde, I., Hecht, J.R., Berlin, J., Allen, B., Bozic, I., Reiter, J.G., Nowak, M.A., et al. (2012). The molecular evolution of acquired resistance to targeted EGFR blockade in colorectal cancers. Nature *486*, 537–540.

2. Engelman, J.A., and Settleman, J. (2008). Acquired resistance to tyrosine kinase inhibitors during cancer therapy. Curr. Opin. Genet. Dev. *18*, 73–79.

3. Holohan, C., Van Schaeybroeck, S., Longley, D.B., and Johnston, P.G. (2013). Cancer drug resistance: an evolving paradigm. Nat. Rev. Cancer *13*, 714–726.

4. Nakata, A., and Gotoh, N. (2012). Recent understanding of the molecular mechanisms for the efficacy and resistance of EGF receptor-specific tyrosine kinase inhibitors in non-small cell lung cancer. Expert Opin. Ther. Targets *16*, 771–781.

5. Sharma, S.V., Bell, D.W., Settleman, J., and Haber, D.A. (2007). Epidermal growth factor receptor mutations in lung cancer. Nat. Rev. Cancer *7*, 169–181.

6. Mitsudomi, T., Morita, S., Yatabe, Y., Negoro, S., Okamoto, I., Tsurutani, J., Seto, T., Satouchi, M., Tada, H., Hirashima, T., et al.; West Japan Oncology Group (2010). Gefitinib versus cisplatin plus docetaxel in patients with non-small-cell lung cancer harbouring mutations of the epidermal growth factor receptor (WJTOG3405): an open label, randomised phase 3 trial. Lancet Oncol. *11*, 121–128.

7. Mok, T.S., Wu, Y.L., Thongprasert, S., Yang, C.H., Chu, D.T., Saijo, N., Sunpaweravong, P., Han, B., Margono, B., Ichinose, Y., et al. (2009). Gefitinib or carboplatin-paclitaxel in pulmonary adenocarcinoma. N. Engl. J. Med. *361*, 947–957.

8. Maemondo, M., Inoue, A., Kobayashi, K., Sugawara, S., Oizumi, S., Isobe, H., Gemma, A., Harada, M., Yoshizawa, H., Kinoshita, I., et al.; North-East Japan Study Group (2010). Gefitinib or chemotherapy for non-small-cell lung cancer with mutated EGFR. N. Engl. J. Med. *362*, 2380–2388.

9. Chan, B.A., and Hughes, B.G.M. (2015). Targeted therapy for non-small cell lung cancer: current standards and the promise of the future. Transl. Lung Cancer Res. *4*, 36–54.

10. Gazdar, A.F. (2009). Activating and resistance mutations of EGFR in non-small-cell lung cancer: role in clinical response to EGFR tyrosine kinase inhibitors. Oncogene *28* (*Suppl 1*), S24–S31.

11. Bach, D.-H., Hong, J.-Y., Park, H.J., and Lee, S.K. (2017). The role of exosomes and miRNAs in drug-resistance of cancer cells. Int. J. Cancer *141*, 220–230.

12. Bach, D.-H., and Lee, S.K. (2018). Long noncoding RNAs in cancer cells. Cancer Lett. *419*, 152–166.

13. Bach, D.-H., Park, H.J., and Lee, S.K. (2017). The dual role of bone morphogenetic proteins in cancer. Mol. Ther. Oncolytics *8*, 1–13.

14. Cho, Y.E., Kim, S.H., Lee, B.H., and Baek, M.C. (2017). Circulating plasma and exosomal microRNAs as indicators of drug-induced organ injury in rodent models. Biomol. Ther. (Seoul) *25*, 367–373.

15. Zhou, X., Yuan, P., Liu, Q., and Liu, Z. (2017). LncRNA MEG3 regulates imatinib resistance in chronic myeloid leukemia via suppressing microRNA-21. Biomol. Ther. (Seoul) *25*, 490–496.

16. Bartel, D.P. (2004). MicroRNAs: genomics, biogenesis, mechanism, and function. Cell *116*, 281–297.

17. Bartel, D.P. (2009). MicroRNAs: target recognition and regulatory functions. Cell *136*, 215–233.

18. Bach, D.-H., Kim, D., Bae, S.Y., Kim, W.K., Hong, J.-Y., Lee, H.-J., Rajasekaran, N., Kwon, S., Fan, Y., Luu, T.T., et al. (2018). Targeting nicotinamide N-methyltransferase and miR-449a in EGFR-TKI-resistant non-small-cell lung cancer cells. Mol. Ther. Nucleic Acids *11*, 455–467.

19. Wang, R.N., Green, J., Wang, Z., Deng, Y., Qiao, M., Peabody, M., Zhang, Q., Ye, J., Yan, Z., Denduluri, S., et al. (2014). Bone Morphogenetic Protein (BMP) signaling in development and human diseases. Genes Dis. *1*, 87–105.

20. Wang, Z., Shen, Z., Li, Z., Duan, J., Fu, S., Liu, Z., Bai, H., Zhang, Z., Zhao, J., Wang, X., and Wang, J. (2015). Activation of the BMP-BMPR pathway conferred resistance to EGFR-TKIs in lung squamous cell carcinoma patients with EGFR mutations. Proc. Natl. Acad. Sci. USA *112*, 9990–9995.

21. Ali, J.L., Lagasse, B.J., Minuk, A.J., Love, A.J., Moraya, A.I., Lam, L., Arthur, G., Gibson, S.B., Morrison, L.C., Werbowetski-Ogilvie, T.E., et al. (2015). Differential cellular responses induced by dorsomorphin and LDN-193189 in chemotherapy-sensitive and chemotherapy-resistant human epithelial ovarian cancer cells. Int. J. Cancer *136*, E455–E469.

22. Emmrich, S., Engeland, F., El-Khatib, M., Henke, K., Obulkasim, A., Schöning, J., Katsman-Kuipers, J.E., Michel Zwaan, C., Pich, A., Stary, J., et al. (2016). miR-139-5p controls translation in myeloid leukemia through EIF4G2. Oncogene *35*, 1822–1831.

23. Zhang, L., Dong, Y., Zhu, N., Tsoi, H., Zhao, Z., Wu, C.W., Wang, K., Zheng, S., Ng, S.S., Chan, F.K., et al. (2014). microRNA-139-5p exerts tumor suppressor function by targeting NOTCH1 in colorectal cancer. Mol. Cancer *13*, 124.

24. Li, Q., Liang, X., Wang, Y., Meng, X., Xu, Y., Cai, S., Wang, Z., Liu, J., and Cai, G. (2016). miR-139-5p inhibits the epithelial-mesenchymal transition and enhances the chemotherapeutic sensitivity of colorectal cancer cells by downregulating BCL2. Sci. Rep. *6*, 27157.

25. Xu, W., Hang, M., Yuan, C.Y., Wu, F.L., Chen, S.B., and Xue, K. (2015). MicroRNA-139-5p inhibits cell proliferation and invasion by targeting insulin-like growth factor 1 receptor in human non-small cell lung cancer. Int. J. Clin. Exp. Pathol. *8*, 3864–3870.

26. Sun, C., Sang, M., Li, S., Sun, X., Yang, C., Xi, Y., Wang, L., Zhang, F., Bi, Y., Fu, Y., and Li, D. (2015). Hsa-miR-139-5p inhibits proliferation and causes apoptosis associated with down-regulation of c-Met. Oncotarget *6*, 39756–39792.

27. Bae, S.Y., Hong, J.Y., Lee, H.J., Park, H.J., and Lee, S.K. (2015). Targeting the degradation of AXL receptor tyrosine kinase to overcome resistance in gefitinib-resistant non-small cell lung cancer. Oncotarget *6*, 10146–10160.

28. Hao, J., Lee, R., Chang, A., Fan, J., Labib, C., Parsa, C., Orlando, R., Andresen, B., and Huang, Y. (2014). DMH1, a small molecule inhibitor of BMP type i receptors, suppresses growth and invasion of lung cancer. PLoS ONE *9*, e90748.

29. Kim, J.S., Kurie, J.M., and Ahn, Y.H. (2015). BMP4 depletion by miR-200 inhibits tumorigenesis and metastasis of lung adenocarcinoma cells. Mol. Cancer *14*, 173.

30. Chen, L., Yi, X., Goswami, S., Ahn, Y.H., Roybal, J.D., Yang, Y., Diao, L., Peng, D., Peng, D., Fradette, J.J., et al. (2016). Growth and metastasis of lung adenocarcinoma is potentiated by BMP4-mediated immunosuppression. OncoImmunology *5*, e1234570.

31. Fotinos, A., Nagarajan, N., Martins, A.S., Fritz, D.T., Garsetti, D., Lee, A.T., Hong, C.C., and Rogers, M.B. (2014). Bone morphogenetic protein-focused strategies to induce cytotoxicity in lung cancer cells. Anticancer Res. *34*, 2095–2104.

32. Padanad, M.S., Konstantinidou, G., Venkateswaran, N., Melegari, M., Rindhe, S., Mitsche, M., Yang, C., Batten, K., Huffman, K.E., Liu, J., et al. (2016). Fatty acid oxidation mediated by Acyl-CoA synthetase long chain 3 is required for mutant KRAS lung tumorigenesis. Cell Rep. *16*, 1614–1628.

33. Phan, A.N.H., Vo, V.T.A., Hua, T.N.M., Kim, M.K., Jo, S.Y., Choi, J.W., Kim, H.W., Son, J., Suh, Y.A., and Jeong, Y. (2017). PPARγ sumoylation-mediated lipid accumulation in lung cancer. Oncotarget *8*, 82491–82505.

34. Miyares, R.L., Stein, C., Renisch, B., Anderson, J.L., Hammerschmidt, M., and Farber, S.A. (2013). Long-chain Acyl-CoA synthetase 4A regulates Smad activity and dorsoventral patterning in the zebrafish embryo. Dev. Cell *27*, 635–647.

35. Maloberti, P.M., Duarte, A.B., Orlando, U.D., Pasqualini, M.E., Solano, A.R., López-Otín, C., and Podestá, E.J. (2010). Functional interaction between acyl-CoA synthetase 4, lipooxygenases and cyclooxygenase-2 in the aggressive phenotype of breast cancer cells. PLoS ONE *5*, e15540.

36. Sánchez-Martínez, R., Cruz-Gil, S., Gómez de Cedrón, M., Álvarez-Fernández, M., Vargas, T., Molina, S., García, B., Herranz, J., Moreno-Rubio, J., Reglero, G., et al. (2015). A link between lipid metabolism and epithelial-mesenchymal transition provides a target for colon cancer therapy. Oncotarget *6*, 38719–38736.

37. Modica, S., and Wolfrum, C. (2017). The dual role of BMP4 in adipogenesis and metabolism. Adipocyte *6*, 141–146.

38. Qian, S.W., Tang, Y., Li, X., Liu, Y., Zhang, Y.Y., Huang, H.Y., Xue, R.D., Yu, H.Y., Guo, L., Gao, H.D., et al. (2013). BMP4-mediated brown fat-like changes in white adipose tissue alter glucose and energy homeostasis. Proc. Natl. Acad. Sci. USA *110*, E798–E807.

39. Tang, Y., Qian, S.-W., Wu, M.-Y., Wang, J., Lu, P., Li, X., Huang, H.Y., Guo, L., Sun, X., Xu, C.J., and Tang, Q.Q. (2016). BMP4 mediates the interplay between adipogenesis and angiogenesis during expansion of subcutaneous white adipose tissue. J. Mol. Cell Biol. *8*, 302–312.

40. Liang, Y., Liu, J., and Feng, Z. (2013). The regulation of cellular metabolism by tumor suppressor p53. Cell Biosci. *3*, 9.

41. Liu, J., Zhang, C., Hu, W., and Feng, Z. (2015). Tumor suppressor p53 and its mutants in cancer metabolism. Cancer Lett. *356* (2 Pt A), 197–203.

42. Wong, C.C., Wong, C.M., Tung, E.K., Au, S.L., Lee, J.M., Poon, R.T., Man, K., and Ng, I.O. (2011). The microRNA miR-139 suppresses metastasis and progression of hepatocellular carcinoma by down-regulating Rho-kinase 2. Gastroenterology *140*, 322–331.

43. Xian, S., Jilu, L., Zhennan, T., Yang, Z., Yang, H., Jingshu, G., and Songbin, F. (2014). BMP-4 genetic variants and protein expression are associated with platinum-based chemotherapy response and prognosis in NSCLC. BioMed Res. Int. *2014*, 801640.

44. Wood, N.J. (2012). Cancer: Integrated epigenomic analysis sheds light on role of BMP4 in regulating cisplatin sensitivity in gastric cancer. Nat. Rev. Gastroenterol. Hepatol. *9*, 301.

45. Ivanova, T., Zouridis, H., Wu, Y., Cheng, L.L., Tan, I.B., Gopalakrishnan, V., Ooi, C.H., Lee, J., Qin, L., Wu, J., et al. (2013). Integrated epigenomics identifies BMP4 as a modulator of cisplatin sensitivity in gastric cancer. Gut *62*, 22–33.

46. Lombardo, Y., Scopelliti, A., Cammareri, P., Todaro, M., Iovino, F., Ricci-Vitiani, L., Gulotta, G., Dieli, F., de Maria, R., and Stassi, G. (2011). Bone morphogenetic protein

4 induces differentiation of colorectal cancer stem cells and increases their response to chemotherapy in mice. Gastroenterology *140*, 297–309.

47. Voorneveld, P.W., Kodach, L.L., Jacobs, R.J., van Noesel, C.J.M., Peppelenbosch, M.P., Korkmaz, K.S., Molendijk, I., Dekker, E., Morreau, H., van Pelt, G.W., et al. (2015). The BMP pathway either enhances or inhibits the Wnt pathway depending on the SMAD4 and p53 status in CRC. Br. J. Cancer *112*, 122–130.

48. Bach, D.H., Kim, S.H., Hong, J.Y., Park, H.J., Oh, D.C., and Lee, S.K. (2015). Salternamide A suppresses hypoxia-induced accumulation of HIF-1α and induces apoptosis in human colorectal cancer cells. Mar. Drugs *13*, 6962–6976.

49. An, Y.J., Xu, W.J., Jin, X., Wen, H., Kim, H., Lee, J., and Park, S. (2012). Metabotyping of the C. elegans sir-2.1 mutant using in vivo labeling and (13)C-heteronuclear multi-dimensional NMR metabolomics. ACS Chem. Biol. *7*, 2012–2018.

50. Bach, D.-H., Liu, J.-Y., Kim, W.K., Hong, J.-Y., Park, S.H., Kim, D., Qin, S.N., Luu, T.T., Park, H.J., Xu, Y.N., and Lee, S.K. (2017). Synthesis and biological activity of new phthalimides as potential anti-inflammatory agents. Bioorg. Med. Chem. *25*, 3396–3405.

51. Um, S., Bach, D.-H., Shin, B., Ahn, C.-H., Kim, S.-H., Bang, H.-S., Oh, K.B., Lee, S.K., Shin, J., and Oh, D.C. (2016). Naphthoquinone–oxindole alkaloids, coprisidins A and B, from a gut-associated bacterium in the dung beetle, copris tripartitus. Org. Lett. *18*, 5792–5795.

52. Kim, W.K., Bach, D.-H., Ryu, H.W., Oh, J., Park, H.J., Hong, J.-Y., Song, H.H., Eum, S., Bach, T.T., and Lee, S.K. (2017). Cytotoxic activities of Telectadium dongnaiense and its constituents by inhibition of the Wnt/β-catenin signaling pathway. Phytomedicine *34*, 136–142.